Hyperspectral Imagery Radiometry Improvements for Visible and Near-Infrared Climate Studies

G. Kopp, G. Drake, J. Espejo, D. Harber, K. Heuerman, A. Lieber, P. Pilewskie, and P. Smith
Laboratory for Atmospheric and Space Physics
Univ. of Colorado
Boulder, CO USA

Abstract — **We describe a new method to improve radiometric accuracy for spaceborne Earth-viewing hyperspectral imaging to help achieve CLARREO mission benchmark measurements of climate in the shortwave spectral region by using on-orbit cross-calibrations to spectral solar irradiances in the near-ultraviolet to near-infrared. Unlike traditional solar diffuser-based calibrations, the methods described here utilize direct observations of the Sun. Maintaining low uncertainties in the ratio of measured incoming to outgoing Earth radiances establishes a benchmark climate record and transfers solar irradiance calibrations to Earth-viewing spatial/spectral instrumentation. A visible and near-infrared hyperspectral imager with integrated solar attenuation methods to demonstrate and quantify the accuracies to which this calibration transfer can achieve end-to-end on-orbit radiometric calibrations and long-term stability corrections is described.**

Keywords — hyperspectral imaging; radiometry; climate; solar irradiance; CLARREO

I. INTRODUCTION

The most fundamental driver of climate on Earth is the long-term balance between the rate radiative energy from the Sun is absorbed by the Earth system and the rate that the Earth emits radiation to space. Highly accurate records of the incident and reflected radiances are required for monitoring climate change, for testing the predictive capabilities of atmospheric climate models, and for linking measurements made in the present epoch with future measurements by using stable and traceable on-orbit references.

Climate studies require measurements of the reflected shortwave radiation from the Earth's atmosphere and surface at high accuracy (<0.2%, k=1) relative to the incident solar radiation to establish benchmark climate data records. These accuracies must not only be achieved pre-launch from ground calibrations, but must be maintained on-orbit. Although such radiometric accuracies exceed those of any heritage Earth-observing remote sensing instrument, the calibration approach described herein establishes a path where the required accuracies of incoming and outgoing radiances can not only be achieved, but also tracked and validated on-orbit across the Earth-reflective spectral region. These improvements to the on-orbit SI-traceable accuracy of the solar radiation reflected or scattered by the Earth's surface and atmosphere are intended to achieve the desired benchmark levels for the National Research Council's 2007 Decadal Survey's [1] Climate Absolute Radiance and Refractivity Observatory (CLARREO) mission by utilizing direct measurements of spectral solar radiances. These radiances can be spatially integrated to give spectral solar irradiance, which provides SI-traceability via the upcoming NOAA-funded CLARREO TSIS spectral solar irradiance measurements.

Tying an Earth-viewing hyperspectral imager to solar irradiance establishes a common reference to both the Sun and Earth-viewing sensors, thus removing a potential common-mode source of uncertainty relating incident solar and reflected Earth radiation. This technology enables the creation of a climate data record that can be linked to future observations and thus establishes a benchmark for climate.

II. SOLAR SPECTRAL CROSS-CALIBRATIONS

Traditional accuracies of remote sensing instruments in the 320-2300 nm spectral region rely on thorough ground calibrations to achieve absolute accuracy and an on-orbit tracking method to diagnose relative changes after launch. Flight stimulus lamps, solar-viewing diffuser plates, lunar observations, and Earth-based vicarious calibrations allow on-orbit tracking or cross-calibrations. These methods achieve accuracies at the ~2% level, being limited by lamp stability, diffuser plate scatter properties, lunar spectral reflectance knowledge, or models of atmospheric transmission ([2]-[9]).

The Earth-viewing hyperspectral imager described directly views the Sun as a calibration source. This imager primarily observes the Earth at nadir, and intermittently scans the Sun using optically integrated calibrated attenuators to establish a relative benchmark of incident radiation. Variations in solar irradiances are smaller and better known than any Earth-based target observed through the atmosphere or any on-board radiance source, enabling inter-comparisons between non-overlapping instruments on decadal time scales. The solar stability and spectral profile plus the ability to observe the Sun from nearly any spacecraft orbit make this source a suitable cross-calibration target for an imager measuring Earth-reflected radiation at high accuracy. The accuracy to which the spectral solar irradiances can be transferred to the imager in its un-attenuated Earth-viewing configuration depends on the calibration accuracies of the attenuators enabling direct solar-viewing.

To directly observe the Sun, the hyperspectral imager must attenuate the solar signal by nearly 10^{-5} to match the typical levels of Earth-reflected radiances (see the spectra in Fig. 1, computed using MODTRAN4 [3]). The imager is designed to

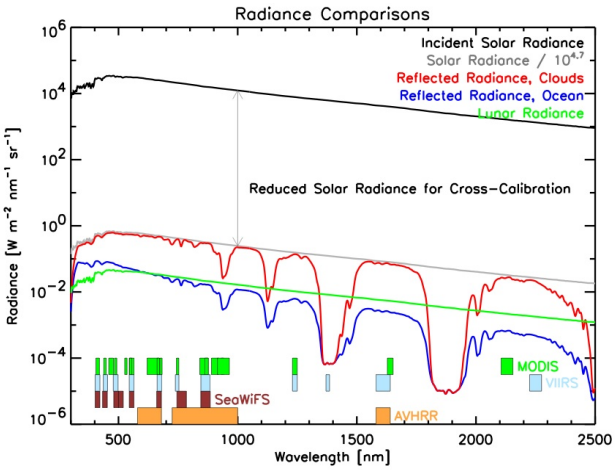

Fig. 1: Solar radiances are 4.7 orders of magnitude greater in intensity than the brightest Earth radiances (red). Darker Earth (blue) and lunar radiances (green) are lower by yet another order of magnitude.

1) scan the Sun and acquire spectral solar radiance measurements, and 2) ensure that the spectral irradiance-to-imager calibration transfer via the selected attenuation methods does not introduce additional uncertainties that exceed the imager's intended 0.2% radiometric accuracy. These requirements are achieved using three methods of radiance attenuation for solar viewing: smaller entrance aperture areas, shorter integration times, and optical filters. These attenuation techniques are utilized (albeit to a lower level of accuracy) on the SOLar STellar Irradiance Comparison Experiment flown on UARS and SORCE [11] to acquire both solar and stellar observations differing in intensity by 10^{-9}. The purpose of the current project is to demonstrate these methods for the higher levels of radiometric accuracy needed for Earth climate studies in the visible and near-infrared.

III. Hyperspectral Imager Design

The hyperspectral imager used in this project to demonstrate the solar cross-calibration approach is designed to meet the requirements given in Table 1 from a nominal 700-km orbit. These specifications enable the imager to acquire the spatial range (>100-km) for adequate sampling of the Earth needed for long-term climate studies, while the 2.5-arcmin (0.5-km ground IFOV) spatial resolution enables identification of select physical causes of climate change. While this prototype imager is not intended to cover the entire 320 to 2300 nm spectral range desired for CLARREO climate studies, the solar attenuation methods demonstrated across the more limited spectral range in this project are extendable to longer wavelengths.

The enabling technologies to be proven involve the highly accurate solar attenuation methods; the hyperspectral imager itself is fairly conventional, and is based on an Offner spectrometer fed by a three mirror anastigmat (TMA). The attenuation methods are selected via filter wheels placed in the pupil plane prior to the TMA or integrated into the spectrometer's focal plane array (FPA).

Table 1: Hyperspectral Imager Requirements

Parameter	Value	Units
Spatial Resolution	0.5	km
Spatial Range (cross-track)	200	km
Wavelength (min)	300	nm
Wavelength (max)	1050	nm
Spectral Resolution	10	nm
Relative Std Uncertainty	0.2	%

A 2-cm diameter entrance aperture for Earth observations is sufficient for the required signal-to-noise across the spectrum for the darker Earth scenes at the 14-Hz frame rates needed to achieve the slit-limited 2.5-arcmin IFOV spatial resolution from low Earth orbit. This NIST-calibrated precision diamond turned knife edge circular aperture is located in the pupil plane prior to the TMA and is selectable via a rotating aperture filter wheel.

An overview of the optical-mechanical layout is shown in Fig. 2. The f/3.56 TMA is an all-reflective design using diamond turned Al mirrors for achromatic performance across the broad spectral range. This images the intended 200-km x 0.5-km ground swath onto the 2.6 cm x 71 µm slit, which is re-imaged 1:1 and dispersed by the Offner's holographic grating onto a 2-D spatial/spectral FPA. Baffles are designed to reduce stray light to 10^{-5}. An optional orthogonal mounting orientation of the spectrometer relative to the TMA (not shown in figure) reduces the instrument's polarization sensitivity. Preliminary optical tests of the integrated TMA and Offner spectrometer indicate the desired performance goals have been achieved with this prototype.

IV. Attenuation Techniques

Attenuations of $10^{-4.7}$ reduce spectral solar radiances to levels typical of Earth scenes (see Fig. 1). Three attenuation methods described below are incorporated into and demonstrated on the hyperspectral imager. Table 2 provides an example combination of these methods that achieves the needed net solar attenuation while limiting individual expected uncertainties so they combine to maintain the desired overall ~0.2% accuracy. Balancing the amount of attenuation from each method against that method's uncertainties, determined analytically and via testing, allows selection of the optimal amount of attenuation applied via each method.

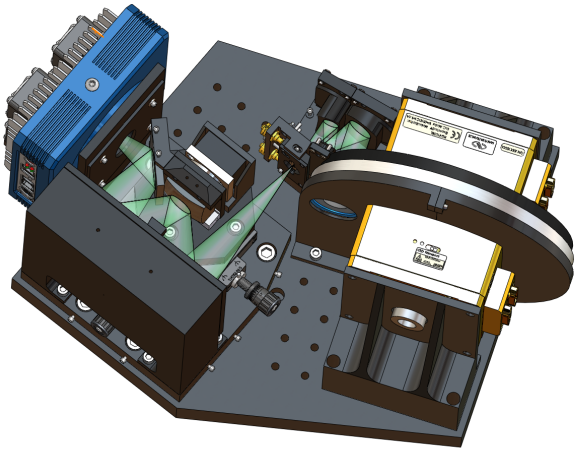

Fig. 2: Optical mechanical layout includes separate attenuation aperture and filter wheels (right), TMA (top center), Offner spectrometer (lower left), and FPA (upper left).

TABLE 2: ESTIMATED ATTENUATION METHOD UNCERTAINTIES

Parameter	Value	Attenuation Amt. (Log)	Uncertainty
Aperture	2 cm/500 μm	3.2	0.14%
Aperture Ratio	*1600.0*	*3.2*	*0.08%*
Diffraction		-	*0.10%*
Underfilled Optics		-	*0.05%*
Integration Time	0.07/0.002 s	0.6	0.09%
Elect. Integration Time	17 ms min	*0.6*	*0.09%*
Mech. Shutter Time	360 μs min	*0.0*	*0.00%*
Filter	ND 1	0.9	0.05%
Lunar Meas. Accuracy	meas. noise		*0.02%*
Underfilled Optics			*0.03%*
Surface Reflections	1° tilt		*0.03%*
Linearity	0.05%/10^2		*0.02%*
Linearity of Signal Levels	-	-	0.05%
Noise	-	-	0.10%
Polarization	0.25%	-	0.05%
Total		4.7	0.21%

A. Aperture Ratio

The solar radiance can be reduced by ~10^{-3} by placing a small precision aperture in the instrument's pupil plane. The ratio of this aperture's geometric area to that of the larger precision aperture used for Earth viewing determines the attenuation level after applying corrections for diffraction. NIST calibrations of aperture areas achieve the levels of accuracy needed for substantial attenuation with this method.

Apertures selected are intended to provide an attenuation of $10^{-3.2}$ using a 2-cm diameter aperture for Earth viewing and a 500-μm aperture for viewing the Sun. NIST quotes a calibration uncertainty of 0.08% for the smaller aperture area, which dominates the aperture ratio uncertainty as the larger aperture can be calibrated to 0.005%. Loss of light by diffraction from the smaller solar-viewing aperture limits this attenuation method's accuracy. This is partly corrected analytically (i.e. large-angle diffraction that misses the spectrometer entrance slit is calculable with ~10% accuracy) and partly by direct measurement (near-angle diffraction that strikes the slit and thus the detector is measured). Diffraction contributes 0.1% uncertainty to the aperture ratio attenuation method for the selected aperture sizes (see Table 2), and limits the use of even smaller apertures to achieve greater attenuations via this method. Because the TMA optics are filled differently by the two apertures, there is an additional small uncertainty that will be quantified by testing but is expected to be <0.05%.

B. Integration Times

Decreased detector integration times will lower the signals measured when observing the Sun, with the ratio of Sun- to Earth-viewing integration times providing the precise attenuation level. Integration times are specified via detector array readout control, so this attenuation method relies purely on electronic timing, which is very accurate and stable; mechanical shutters are not needed.

A CMOS FPA provides short integration times and an electronic shutter capability to eliminate image smear during readout, which is a limiting issue with CCDs for this application despite their superior signal-to-noise. Frame rates of greater than 600 Hz for the selected CMOS FPA, compared to the nominal Earth-observing 14 Hz, give potential attenuations of <10^{-1} using variable integration times. The frame rate can be further increased by using a region of interest readout of the CMOS FPA. Since the Sun only fills a small portion of the array, added attenuation for solar viewing is possible should further intensity reduction be necessary.

C. Filters

Broadband spectral transmissive filters placed in the pupil plane for solar viewing provide additional attenuation. Filters are generally not stable to the accuracies required here, but these will be calibrated on-orbit using the moon, which has comparable radiance to the Earth (see Fig. 1). Filter attenuation calibrations utilizing lunar observations, which are stable over the few minutes needed to acquire measurements with and without filters in place, have the added benefit that the solar attenuation filters are calibrated by and used for sources (the Moon and the Sun) subtending nearly identical angular extents.

Filters are used for additional attenuations of ~10^{-1}. Dynamic range of the imager limits much greater attenuations from this method. No single filter covers the entire spectral region uniformly, so different filters are used for attenuations in different portions of the spectrum, although they are calibrated and used individually. The filters are not staged in series to avoid complications from secondary images. Translating the filters slightly in the pupil plane characterizes filter uniformity to verify that the area illuminated by the under-filling solar aperture has attenuation representative of the larger area used during lunar calibrations. The uncertainties associated with these effects are filter-dependent and difficult to model, so they will be demonstrated by lab measurements for the selected filters.

V. TEST FACILITY VALIDATES ACCURATE ATTENUATIONS

The solar cross-calibration approach described relies on applying accurately known attenuations to enable direct imaging of the Sun. To prove that each attenuation method gives the expected radiance reduction while remaining within the ~0.2% net uncertainty, as in Table 2, the attenuation methods are independently and collectively validated using a test facility to illuminate the hyperspectral imager with a uniform incident light beam controllable over large dynamic range.

By precisely monitoring incident beam power while increasing radiances to exactly compensate for successive levels of attenuation applied in the imager, the actual level of attenuation can be determined. This is done for each attenuation method individually and for the three methods together in any desired combination to validate the expected attenuations and uncertainties. This validation capability requires the ability to vary the incident beam radiance by at least 5 orders of magnitude and to monitor it with high precision over that dynamic range.

An 18-W 532-nm Verdi laser provides sufficiently high power to create spectral solar radiance levels even after the beam is expanded to provide uniform illumination across the imager's Earth-viewing 2-cm entrance aperture. The beam power is stabilized to ~0.03% over a few hours. Direct beam expansion after a 5-μm pinhole provides a uniform radiance at spectral solar power levels at the imager's entrance aperture

and is far more efficient than conventional approaches of using an integrating sphere to create a beam of uniform intensity.

The beam incident on the imager is monitored by a trap photodiode and amplifier system calibrated across the needed dynamic range. NIST has calibrated the linearity of this custom silicon trap photodiode detector and its paired transimpedance amplifier across >6 orders of magnitude in incident optical power to an accuracy of <0.07% using their Beamcon III facility [12]. The photodiode system is then used to precisely monitor changes in the applied laser power when verifying the imager's attenuation accuracies.

Construction and checkout of this test facility is nearly complete, and tests of the integrated hyperspectral imager and attenuation methods will be starting shortly to validate the attenuation accuracies described.

VI. SUMMARY

Integrated attenuation methods enabling direct spectral solar radiance measurements with an Earth-viewing hyperspectral imager allow observations of incoming and outgoing Earth radiances and cross-calibrations from SI-traceable spectral solar irradiances. The on-orbit calibrations enabled by directly viewing the Sun, which has smaller and better known variations than any Earth-based target observed through the atmosphere or any on-board radiance source in the visible and near-infrared spectral region, allows improved radiometric accuracies required for future climate missions such as CLARREO. This paper describes three attenuation methods integrated into a hyperspectral imager intended to demonstrate that solar cross-calibrations can be achieved with the needed levels of radiometric accuracy for on-orbit imager calibrations and stability tracking to enable long-term Earth climate studies based on visible and near-infrared radiance measurements.

REFERENCES

[1] "Earth Science and Applications from Space: National Imperatives for the Next Decade and Beyond," Committee on Earth Science and Applications from Space: A Community Assessment and Strategy for the Future, National Research Council, ISBN: 0-309-66714-3, (2007).

[2] Beiso, D., "Overview of Hyperion On-Orbit Instrument Performance, Stability, and Artifacts," aipr, p. 95, 31st Applied Imagery Pattern Recognition Workshop (2002).

[3] Dinguirard, M., and P. Slater, "Calibration of Space-Multispectral Imaging Sensors: A Review," *Remote Sens. of Environ.*, 68, 194–205 (1999).

[4] Green, R.O., M.L. Eastwood, C.M. Sarture, T.G. Chrien, M. Aronsson, B.J. Chippendale, J.A. Faust, B.E. Pavri, C.J. Chovit, M. Solis, and M.R. Olah, "Imaging Spectroscopy and the Airborne Visible/Infrared Imaging Spectrometer (AVIRIS)", *Remote Sens. of Environ.* 65, 227–248 (1998).

[5] Guenther, B., W. Barnes, E. Knight, J. Barker, J. Harnden, R. Weber, M. Roberto, G. Godden, H. Montgomery, and P. Abel, "MODIS Calibration: A brief review of the strategy for the at-launch calibration approach." *J. Atmos. Oceanic. Technol.*, 13, 274-285 (1996).

[6] T. C. Stone and H. H. Kieffer, "Use of the Moon to support on-orbit sensor calibration for climate change measurements," Proc. SPIE 6296 (2006).

[7] Xiong, X., N. Che, and W. Barnes, "Terra MODIS on-orbit spatial characterization and performance," *IEEE Transactions on Geoscience and Remote Sensing,* 43 (2005a).

[8] Xiong, X., N. Che and W.L. Barnes, "Five-year of Terra MODIS on-orbit spectral characterization," *Proc. SPIE* — Earth Observing Systems X, 5882 (2005b).

[9] Xiong, X., H. Erives, S. Xiong, X. Xie, J. Esposite and J. Sun et al., "Performance of Terra MODIS solar diffuser and solar diffuser stability monitor," *Proc. SPIE* — Earth Observing Systems X, 5882 (2005c).

[10] Berk, A., Anderson, G. P., Acharya, P. K., Chetwynd, J. H., Bernstein, L. S., Shettle, E. P., Matthew, M. W., and Adler-Golden, S. M., MODTRAN4 User's Manual, Air Force Research Laboratory, Space Vehicles Directorate, Air Force Materiel Command, Hanscom AFB, MA, (2000).

[11] McClintock, E.W., G.J. Rottman, and T.N. Woods, "Solar-Stellar Irradiance Comparison Experiment II (SOLSTICE II): Instrument Concept and Design," *Solar Physics*, **230**, 225-258 (2005).

[12] Thompson, A., and H. Chen, "Beamcon III: A Linearity Measurement Instrument for Optical Detectors," *J. Res. Natl. Inst. Stand. Technol*., 99, 751-755 (1994).